

Interferometry for the LISA technology package LTP: an update

G Heinzel¹, J Bogenstahl², C Braxmaier^{3,6}, K Danzmann¹, A Garcia¹, F Guzman¹, J Hough², D Hoyland⁵, O Jennrich⁴, C Killow², D Robertson², Z Sodnik⁴, F Steier¹, H Ward² and V Wand¹

¹ Max-Planck-Institut für Gravitationsphysik (Albert-Einstein-Institut) and University of Hannover, Callinstraße 38, D-30167 Hannover, Germany

² University of Glasgow, UK

³ EADS Astrium GmbH, Immenstaad, Germany

⁴ ESTEC, Noordwijk, The Netherlands

⁵ University of Birmingham

E-mail: gerhard.heinzel@aei.mpg.de

Abstract. This paper gives an update on the status of the LISA technology package (LTP) which is to be launched in 2009 by ESA as a technology demonstration mission for the space-borne gravitational wave observatory LISA. The dominant noise source in the interferometer prototype has been investigated and improved such that it is now comfortably below its budget at all frequencies.

1. Introduction

The LISA Pathfinder (LPF) mission [1, 2, 3] will be launched in 2009 by ESA. It will contain a European LISA Technology Package (LTP) and a similar US-package called DRS. The purpose of the mission is to:

- Demonstrate the free fall of the test mass within one order of magnitude of the LISA specifications: The goal for LTP is $3 \times 10^{-14} \text{ ms}^{-2}/\sqrt{\text{Hz}}$ at 3 mHz.
- Verify in orbit the functionality and performance of:
 - the drag-free system,
 - operation of the test mass as a mirror of a precision interferometer,
 - the μN thrusters,
 - capacitive sensors and actuators,
 - caging mechanism,
 - ultra-stable interferometer with pm accuracy.

The LTP is currently being built by a large team including Albert-Einstein-Institut Hannover, Germany, University of Trento, Italy, University of Glasgow, UK, University of Birmingham, UK, Imperial College London, UK, ETH Zürich, Switzerland, CNES, Paris, France, DLR, Germany, ASI, Italy, SRON, The Netherlands, IEEC, Barcelona, Spain, with ESA/ESTEC in Noordwijk

⁶ Present address: University of Applied Sciences, Konstanz, Germany.

as the leading agency and EADS Astrium GmbH Immenstaad, Germany as industrial prime contractor.

Figures 1 and 2 show the acceleration noise budget for LISA and LTP, and the present performance of the interferometer prototype. The design and construction of the interferometer is described in References [4], [5], [6], [7] and [8].

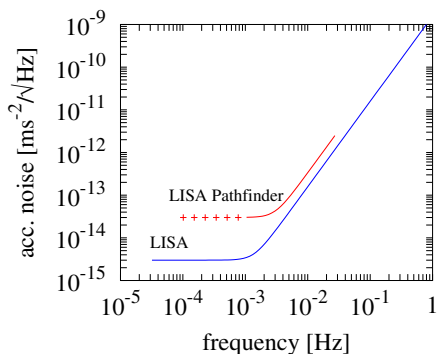


Figure 1. Acceleration noise requirements for LISA and LTP.

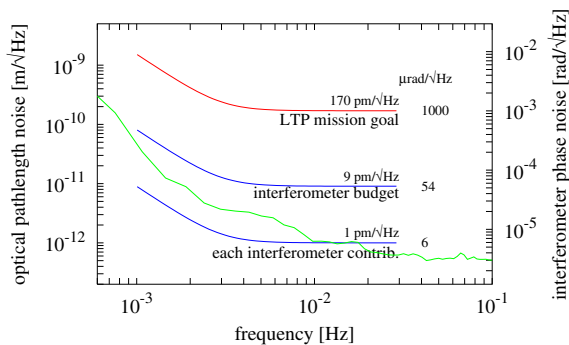


Figure 2. LTP requirements, interferometer budget and current performance of interferometer prototype.

2. Phasemeter

Recently the previous PC-based phasemeter has been replaced by a breadboard similar to the flight model. The phase is measured in many channels simultaneously by digitizing the photocurrent and performing a single-bin discrete Fourier transform (SBDFT), i.e. multiplying the time series by a sine- and cosine-wave of the correct frequency. This simple, but time-consuming step is done in dedicated hardware (FPGA). Figure 3 shows a block diagram of the FPGA, and Figure 4 the measured noise of the phasemeter (lowest curve). Our breadboard uses one 18-bit A/D converter at 800 kHz sampling frequency per channel, while the flight model (being built in Birmingham) will use 16-bit converters at 50 kHz or 100 kHz.

3. Sideband-induced noise

The most important noise source in the interferometer has recently been studied in detail. It is caused by spurious sidebands on the light that are in turn caused by RF crosstalk between the two nearby RF frequencies that drive the acousto-optical modulators. In a simplified sketch of the interferometer (Figure 5), we introduce the phases

$$\Delta_F = \frac{2\pi}{\lambda}(L_1 - L_2), \quad \Delta_R = \frac{2\pi}{\lambda}(L_{1R} - L_{2R}), \quad \text{and} \quad \Delta_M = \frac{2\pi}{\lambda}(L_{1M} - L_{2M}),$$

which represent differential pathlength fluctuations of the unstable part (mostly the fibers), the (stable) reference interferometer and the measurement interferometer, respectively and neglect any static pathlength differences. The pathlengths L_{1R} , L_{2R} , L_{1M} and L_{2M} are defined by distances on the ultrastable optical bench, which is constructed by quasi-monolithic hydrocatalysis bonding on a Zerodur baseplate and which is located in a thermally very stable environment such that the fluctuations of these pathlengths are smaller than our measurement goal.

The primary observables thus become

$$\varphi_R = \Delta_F + \Delta_R \quad \text{and} \quad \varphi_M = \Delta_F + \Delta_M.$$

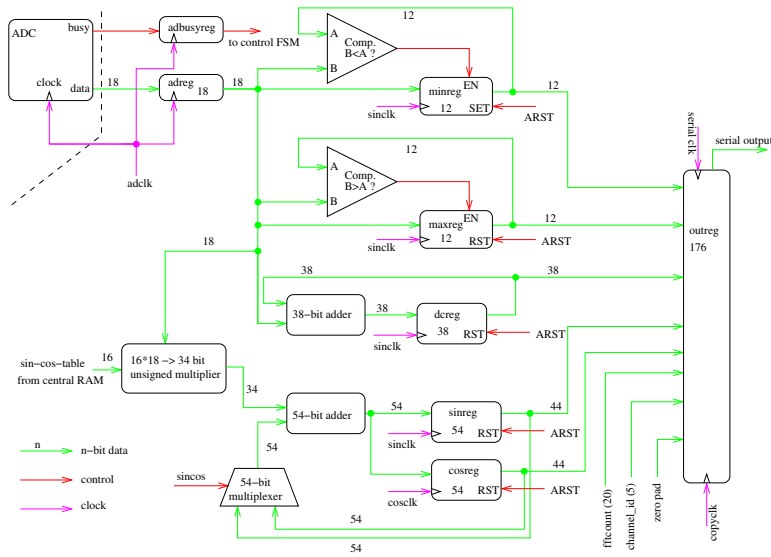


Figure 3. Block diagram of the Hannover breadboard for the FPGA-based phasemeter front end.

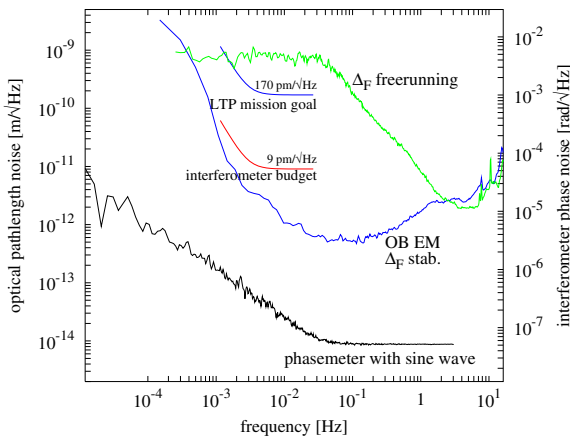


Figure 4. Noise performance of the Hannover phasemeter breadboard. The measured curves show (from top to bottom): Interferometer noise without Δ_F stabilization, a typical noise curve obtained with Δ_F stabilization and laser amplitude stabilization, and the noise of the new phasemeter when driven with a clean sine wave.

The main measurement consists of taking the difference between φ_R and φ_M : $\varphi = \varphi_R - \varphi_M$.

Ideally, Δ_F should cancel and φ should represent the test mass motion Δ_M , provided that the reference path on the optical bench Δ_R is stable. Experimentally, this is true to the mrad (equivalently nm) level. Looking more closely, however, one discovers that φ is not perfectly independent of the fiber pathlength difference Δ_F , even if both Δ_R and Δ_M are stable. Figure 6 shows a measurement of φ , when Δ_F was freely fluctuating, and the uppermost curve in Figure 4 shows the resulting interferometer noise spectrum, which is clearly unacceptable.

Figure 7 shows the spectra of the two AOM driving frequencies with sidebands, which directly translate into the optical spectra of the two light beams. In our breadboard electronic modules (which were built before this problem was discovered), such sidebands are caused by electrical crosstalk between insufficiently shielded VCXO's and 80 MHz power amplifiers.

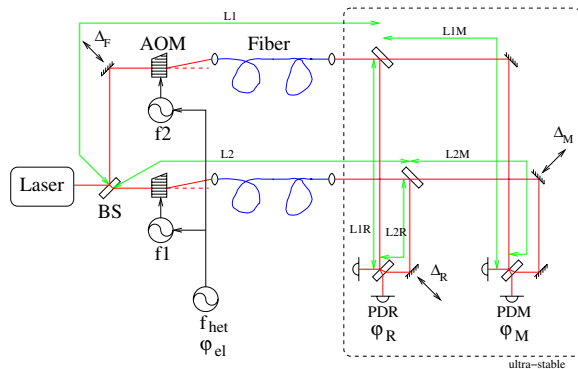


Figure 5. Simplified diagram of a heterodyne interferometric setup, with one ‘measurement’ interferometer and a reference interferometer.

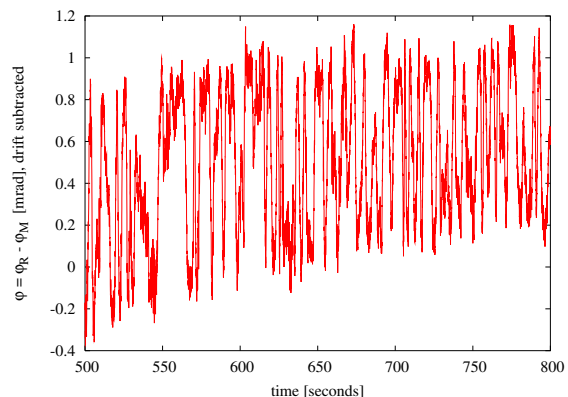


Figure 6. Measured noise caused by Δ_F fluctuations together with sidebands on the light.

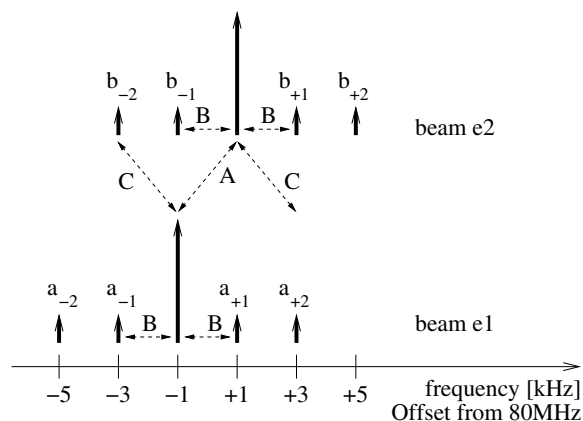


Figure 7. Sidebands on the light and their beat notes. For this illustration, 80 MHz is the average AOM driving frequency, and the heterodyne frequency is 2 kHz. ‘A’ represents the (desired) main beatnote between carrier and carrier. The spurious beatnotes labelled ‘B’ produce an error term that varies as $\sin(\Delta_F)$, while those labelled ‘C’ cause an error $\sim \sin(2\Delta_F)$.

A theoretical analysis [9] of the errors caused by these sidebands has shown that

- The first-order sidebands cause a phase error of the form

$$\delta\varphi = \left\{ \alpha_1 \sin\left(\frac{\varphi_M + \varphi_R}{2}\right) + \alpha_2 \cos\left(\frac{\varphi_M + \varphi_R}{2}\right) \right\} \cdot \sin\left(\frac{\varphi_M - \varphi_R}{2}\right),$$

where α_1 and α_2 are combinations of the amplitudes and phases of the individual sidebands.

- a pair of first-order sidebands that are caused by phase modulation of the RF or light cancel and produce no resulting error.
- first-order sidebands that are caused by amplitude modulation add and produce twice the error of an individual sideband.
- Of the second-order sidebands, only those labelled ‘C’ in Figure 7 produce an error term, which has the form

$$\delta\varphi = \{ \alpha_3 \sin(\varphi_M + \varphi_R) + \alpha_4 \cos(\varphi_M + \varphi_R) \} \cdot \sin(\varphi_M - \varphi_R).$$

Hence it is irrelevant whether the sideband was caused by phase- or amplitude-modulation or occurs as single sideband.

- All error terms scale with the amplitude of the sideband, both in the light and the RF signal. This means that in order to reduce the error (measured in radians) by a factor of 10, the offending sideband needs to be reduced by 20 dB (not 10 dB).

All these predictions have been confirmed by a series of experiments using the breadboards of the optical bench and associated electronics.

Several strategies to mitigate this error have also been investigated:

- Reduction of the offending sidebands: The results described above have led to more stringent requirements on the spectral purity of the AOM unit of the flight model.
- Reducing the fluctuations of Δ_F : This is now routinely used in our breadboards and will also be included in the flight model. For this purpose, the pathlength difference Δ_F between the two unstable optical paths, which is measured by the phasemeter, is actively stabilized using a PZT in the AOM unit.
- Since the analytical form of the error is known, it can be removed by subtraction from corrupted data. Although this has been shown to work in principle and a reduction of the error by a factor of 10 or so was achieved, measuring the coefficients $\alpha_1 \dots \alpha_4$ is difficult in practice, and hence this method is not the baseline.

The analysis and results will be published in more detail in another paper.

4. Conclusions

Using the new phasemeter, active stabilisation of Δ_F and active suppression of the laser amplitude noise, the noise of the interferometer has been reduced to the levels shown in Figures 2 and 4. The remaining noise at low frequencies is mainly due to real motion of the test mirrors, which is caused by thermal fluctuations in the lab. We expect that these fluctuations (as well as the Δ_F fluctuation) will be considerably smaller in the quiet orbit of LPF, and that the interferometer will hence perform considerably better than its requirement, thus enabling LTP to study other noise sources (e.g. of the drag-free system) with high detail and fidelity.

Acknowledgments

Many of the results presented here were obtained under a contract from ESA/ESTEC.

References

- [1] Vitale S et al. 2002 *NUCLEAR PHYSICS B-PROCEEDINGS SUPPLEMENTS* **110** 209–216
- [2] Bortoluzzi D et al. 2003 *CLASSICAL AND QUANTUM GRAVITY* **20** S89–S97
- [3] Anza S et al. 2005 *CLASSICAL AND QUANTUM GRAVITY* **22** S125–S138
- [4] Heinzl G et al. 2003 *CLASSICAL AND QUANTUM GRAVITY* **20** S153–S161
- [5] Heinzl G et al. 2004 *CLASSICAL AND QUANTUM GRAVITY* **21** S581–S587
- [6] Heinzl G et al. 2005 *CLASSICAL AND QUANTUM GRAVITY* **22** S149–S154
- [7] Braxmaier C et al. 2004 *J PROC OF SPIE 5500* 164–173
- [8] Robertson D et al. 2005 *CLASSICAL AND QUANTUM GRAVITY* **22** S155–S163
- [9] Heinzl G et al. 2005 *Investigation of noise sources in the LTP interferometer* Technical note available upon request from the authors.